Journal of Geomatics Vol 9 No. 1April 2015

Assessment of SAR polarimetric decompositions for land cover studies

Bindi P. Shastri[1], R.L. Mehta[2], S. Mohan[3] and Anjana Vyas[1]
[1]Centre for Environment Planning and Technology, Ahmedabad
[2]Advanced Techniques Development Group (ATDG), Space Applications Centre, Ahmedabad
[3]PLANEX/Physical Research Laboratory, Ahmedabad-380059
Email: shastribindy@gmail.com

(Received: Nov 06, 2014; in final form: Apr 16, 2015)

Abstract: One of the main advantages of polarimetric radar data analysis is the possibility of separating and identifying contributions from different types of scatterers in the imaged terrain. For this purpose, received scattering matrix is analyzed using various techniques to extract information about the scattering processes, referred to as "target decomposition". In the present study, full polarimetric L-band ALOS-PALSAR data has been used to generate various decomposition techniques using RAT and PolSARpro software. Polarimetric decomposition techniques like Freeman-Durden, eigen value/ eigen vector, H/A/α and Moriyama decomposition were evaluated for this study. The study area is a desert terrain dominated by agricultural land covering parts of Nagaur district, Rajasthan. Outputs of the decomposition techniques were also analyzed for observing the accuracy of these techniques for each selected land use classes. When considering all classes, maximum accuracy of pixel classification and separability was observed in the case of eigen vector based decomposition, followed by Moriyama decomposition, Freeman Durden decomposition and H/A/α decomposition. This paper is thus an attempt to evaluate the various decomposition techniques based on separability and classification accuracies for optimum utilization of polarimetric SAR data.

Keywords: SAR, Polarimetric decompositions, Land cover class

1. Introduction

Currently, there is a great deal of interest in the use of Polarimetry for radar remote sensing. In this context, an important objective is to extract physical information from the observed scattering of microwaves by surface and volume structures. The polarimetric information of target echo can reflect the geometry, structure and physical characteristic of the former, while polarimetric target decomposition theorems express the average mechanism as the sum of independent elements in order to associate a physical mechanism with each component. Unlike using SAR for information process, target decomposition explores phase message contained in polarimetric SAR data. Polarimetric target decomposition theorems can be used for target classification or recognition (Zhang et al., 2008). Polarimetric SAR data are coherent by nature of the principal of operation, however most often incoherent approaches are chosen for the post processing in order to apply conventional averaging and statistical method. At present, two main classes of decomposition can be identified. One being Coherent decomposition, that deals with decomposition of scattering matrix, while the other being Incoherent decomposition, which deals with decomposition of coherency or covariance matrices. In this paper, incoherent decompositions, based on [C] and [T] matrix have been considered, as the study area is comprised of distributed targets in majority. The scattering matrix [S] is only able to characterize the so-called coherent or pure scatterers. On the contrary, this matrix cannot be employed to characterize, from a polarimetric point of view, the so-called distributed scatterers. This type of scatterers can be only characterized, statistically, due to the presence of speckle noise. Since speckle noise must be reduced, only second order polarimetric representations can be employed to analyze distributed scatterers. These second order matrices prove to be useful since they can better deal with the real case of partially polarized scattered waves. It is worthwhile to introduce them before using them for various decompositions (Das, 2011).

The main purpose of this paper is to evaluate the capability of polarimetric target decomposition algorithms in land use/land cover mapping using full polarimetric L-band SAR data. The decomposition techniques that have been considered for the study are Freeman-Durden decomposition, Moriyama decomposition, eigen vector decomposition and H/A/α decomposition.

1.1 Polarimetric decomposition techniques

Freeman Durden decomposition

The Freeman-Durden approach is based on the decomposition of power reflection matrix of a scatterer. The scattering mechanism of a target or an ensemble of targets can be explained through a 3x3 scattering matrix (the coherency [T] or the covariance [C] matrix) in power domain for monostatic case. The Freeman-Durden decomposition models the covariance matrix as the contribution of three scattering mechanisms (Freeman and Durden, 1998; Lee et al., 2004): (1) Volume scattering where a canopy scatterer is modeled as a set of randomly oriented dipoles, (2) Double-bounce scattering modeled by a dihedral corner reflector and (3) Surface or single bounce scattering modeled by a first-order Bragg surface scatterer.

$$[C] = f_s[C_{surface}] + f_d[C_{double}] + f_v[C_{volume}] \qquad (1)$$

where, the terms *fv*,*f*d and *f*s correspond to the contribution of the volume scattering, double-bounce scattering and surface-like scattering, respectively to the final covariance matrix *[C]*.

According to this model, the measured power P may be decomposed into three quantities:

$$P = P_{surface} + P_{double-bounce} + P_{volume} \quad (2)$$

where,

$$P_s = f_s\left(1+|\beta|^2\right),\quad P_d = f_d\left(1+|\alpha|^2\right),\quad P_v = 8f_v/3$$

Consequently, the scattered power *Pv*, *Pd* and *Ps* were employed to generate a RGBimagetopresent all the color-coded polarimetric information in a sole image.

Assumptions:

-Like-polarized and cross-polarized elements are uncorrelated:

$$\left\langle S_{hh}S_{hv}^{*}\right\rangle \approx \left\langle S_{vv}S_{hv}^{*}\right\rangle \approx 0$$

$$[C] = f_{odd}\begin{bmatrix}|\beta|^2 & 0 & \beta\\ 0 & 0 & 0\\ \beta & 0 & 1\end{bmatrix} + f_{even}\begin{bmatrix}|\alpha|^2 & 0 & \alpha\\ 0 & 0 & 0\\ \alpha & 0 & 1\end{bmatrix} + f_{cross}\begin{bmatrix}|\gamma|^2 & \gamma\rho^{*} & \gamma\\ \gamma\rho^{*} & |\rho|^2 & \rho\\ \gamma & \rho & 1\end{bmatrix} \quad (3)$$

$$\Rightarrow [C] = \begin{bmatrix} f_{odd}|\beta|^2 + f_{even}|\alpha|^2 + f_{cross}|\gamma|^2 & f_{cross}\gamma\rho^{*} & f_{odd}\beta + f_{even}\alpha + f_{cross}\gamma\\ f_{cross}\gamma\rho^{*} & f_{cross}|\rho|^2 & f_{cross}\rho\\ f_{odd}\beta + f_{even}\alpha + f_{cross}\gamma & f_{cross}\rho & f_{odd} + f_{even} + f_{cross}\end{bmatrix} \quad (4)$$

where, $\rho = \frac{S_{hv}}{S_{vv}}$ $\rho = \frac{S_{hv}}{S_{vv}}$

According to this model, the measured power P may be decomposed into three quantities:

$$P = P_{odd} + P_{even} + P_{cross}$$

where,

$$P_{odd} = f_{odd}\left(1+|\beta|^2\right),\quad P_{even} = f_{even}\left(1+|\alpha|^2\right),\quad P_{cross} = f_{cross}\left(1+|\gamma|^2+2|\rho|^2\right) \quad (5)$$

Eigen value based decomposition

Cloude and Pottier (1996) have proposed a polarimetric decomposition theorem based on the Eigen value – eigenvector decomposition of the coherency matrix into elementary mechanisms (i.e. single, double-bounce and volume scattering) in order to identify the global mean scattering mechanism. The coherency matrix [*T*] is obtained from an ensemble of scattering matrix samples [*Si*] by forming the Pauli scattering vectors, as discussed above:

$$\langle [T] \rangle = \left\langle \vec{k}_{P_i} \cdot \vec{k}_{P_i}^{+} \right\rangle = \begin{bmatrix} \left\langle |S_{hh}+S_{vv}|^2 \right\rangle & \left\langle (S_{hh}+S_{vv})(S_{hh}-S_{vv})^{*} \right\rangle & 2\left\langle (S_{hh}+S_{vv})S_{hv}^{*} \right\rangle\\ \left\langle (S_{hh}-S_{vv})(S_{hh}+S_{vv})^{*} \right\rangle & \left\langle |S_{hh}-S_{vv}|^2 \right\rangle & 2\left\langle (S_{hh}-S_{vv})S_{hv}^{*} \right\rangle\\ 2\left\langle (S_{hh}+S_{vv})^{*}S_{hv} \right\rangle & 2\left\langle (S_{hh}-S_{vv})^{*}S_{hv} \right\rangle & 4\left\langle |S_{hv}|^2 \right\rangle \end{bmatrix} \quad (6)$$

-The cross-polarized response is generated by the volume scatterer only.

This method is based on simple physical scattering mechanism (surface scattering, double bounce scattering, and volume scattering). The contribution of each of the three scattering mechanisms to the total power are shown for each pixel usually with surface scattering as red, volume scattering as green, and double bounce scattering as blue (Das, 2011).

Moriyama decomposition

In case of Moriyama decomposition (Moriyama *et al.* 2005):

-For urban area, the condition $\left\langle S_{hh}S_{hv}^{*}\right\rangle \approx \left\langle S_{vv}S_{hv}^{*}\right\rangle \approx 0$ does not hold. Hence $\left\langle S_{hh}S_{hv}^{*}\right\rangle \neq 0\ \left\langle S_{vv}S_{hv}^{*}\right\rangle \neq 0$

-In urban area the thin wire and dihedral corner reflector also produce cross polarized response.

The idea of the eigenvector approach is to use the diagonals of [*T*] obtained from a partial scatterer, which is in general of rank 3, in order to represent it as the non-coherent sum of three deterministic orthogonal scattering mechanisms. Each of the three scattering contributions, expressed in terms of coherency matrices [*T1*], [*T2*] and [*T3*], is obtained from the outer product of one eigenvector and weighted by its appropriate eigen value.

$$[T] = [T_1] + [T_2] + [T_3] \quad (7)$$

According to a simplified interpretation, for natural surface scatterers the first scattering component [T_1] represents the dominant anisotropic surface scattering contribution. The second and third components, [T_2] and [T_3], represent secondary dihedral and multiple scattering contributions, respectively. The eigen decomposition of the coherency matrix is also referred as H/A/α decomposition.

H/A/α parameter

The interpretation of the H/A/α decomposition is performed by studying the value of the eigen values-eigen vectors of the decomposition. A given eigen value corresponds to the associated scattered power to the corresponding eigenvector. Consequently, the eigen value gives the importance of the corresponding eigenvector or scattering mechanism. The ensemble of scattering mechanisms is studied by means of the entropy H, alpha angle (α) and the anisotropy A. The alpha angle has a useful range of 90° and corresponds to a continuous change from surface scattering in the geometrical optics limit (α = 0°) through surface scattering under physical optics to the Bragg surface model, encompassing dipole scattering (α = 45°) and moving into double bounce scattering mechanisms between two dielectric surfaces, finally reaching dihedral scattering from metallic surfaces at α = 90° (Das, 2011).

2. Study area and data set

For this study, a part of Nagaur district in Rajasthan, India, has been considered, with its central geographic coordinate being 73.99˚ and 26.94˚. The study area is a desert terrain comprising mainly of agricultural land, scattered waste lands, open scrubs and urban clusters. ALOS- PALSAR data acquired on 4th December 2008 has been used. Full polarimetric SLC (Single look complex) data processed at level 1.1 A was obtained. The data was acquired at 21.5º incidence angle in the ascending mode with 30 m spatial resolution and 30 km swath. The land cover classes were confirmed using near synchronous optical IRS LISS-III data, of 25th November, 2008.

3. Methodology

The methodology adopted included generation of coherency (T3) matrix and covariance matrix (C3) from L-band full polarimetric ALOS PALSARdata, using PolSARpro software. Speckle suppression using Lee-Sigma filter with 5x5 window size was done. This is followed by generation of decomposed images from the former over a part of Nagaur district using RAT software. The decomposition techniques considered for the study are Freeman Durden decomposition, Moriyama decomposition, eigen vector decomposition, and H/A/α decomposition. Identification of various land use classes from the processed full polarimetric quad-pol data were done using corresponding IRS LISS-III optical data and the ground truth information. Once the classes were identified, training windows were marked and signatures for the four land use classes (namely settlement, Bajra crop, agricultural fallow land and scrub) were extracted. Based on the training windows selected, contingency matrix, based on Maximum likelihood parametric rule and separability (Jeffries-Matusita distance) of the four land use classes were generated and evaluated for each of the decomposition techniques. From the observations made in the above step, decomposition techniques were prioritized based on the classification accuracy and separability for each of the land use classes along with overall land use classification for full polarimetric data.

For the evaluation of different decomposition techniques for land use classification, ALOS PALSAR image covering various land use classes was selected. Figure 1(a) shows ALOS PALSAR multi-polarimetric

Figure 1: (a) FCC of L-band PALSAR image (b) LISS-III FCC corresponding to (a)

backscattering image, wherein urban classes are represented by white to bright yellow, crops by green tones, scrubs by black tones and fallow areas by purple to pink colour. IRS LISS-III image (Figure 1 b) was used for identifying these classes. Classification accuracy of land use classes is shown in Table-1. The overall accuracy of classification was 93.50%, and the overall average pixel separability within the selected classes was 1307 (Jeffries-Matusita distance).

Table 1: Overall classification accuracy (%) of selected land use classes (for Fig. 1)

Classes	Classification accuracy (%)
Urban	98.09
Crop	95.47
Scrub	93.83
Fallow Land	86.62

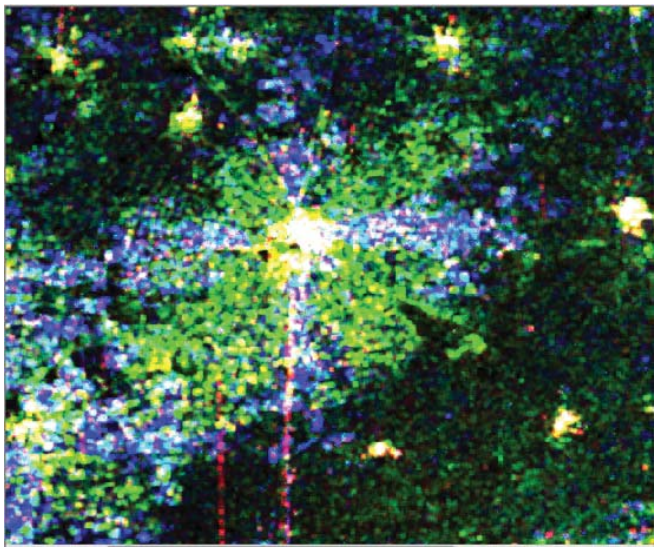

Figure 2: Freeman Durden decomposition (Double Bounce: Volume: Surface)

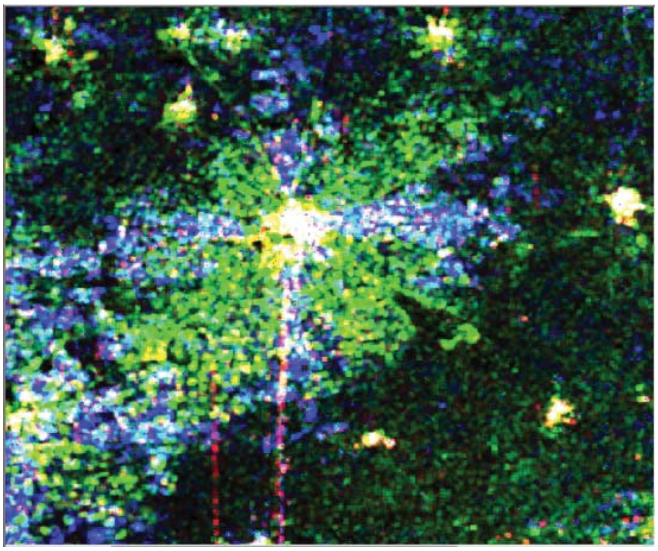

Figure 3: Moriyama decomposition (Double Bounce: Volume: Surface)

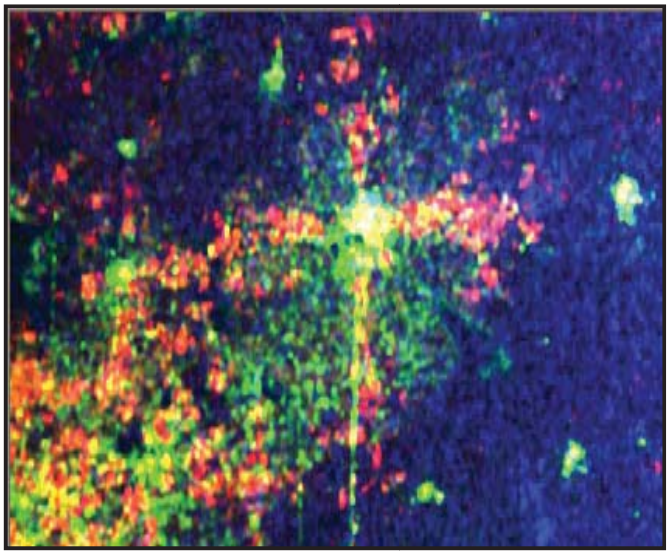

Figure 4: Eigen vector decomposition (Anisotropy: Alpha: Entropy)

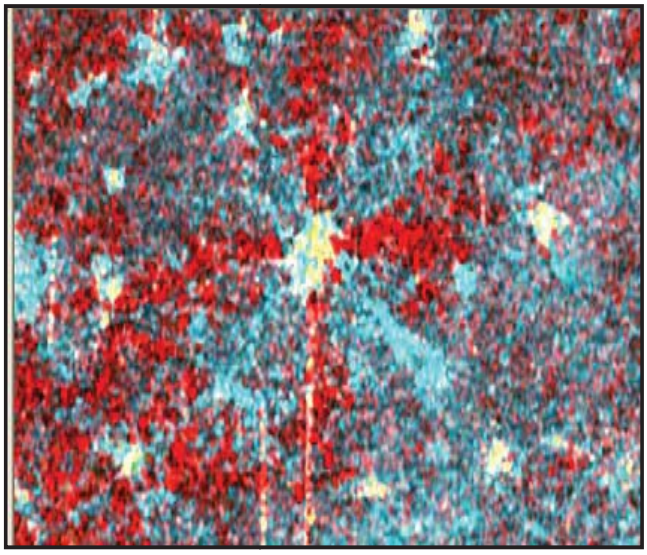

Figure 5: H/A/α decomposition (Eigen value 1: Eigen value 2: Eigen value 3)

Table 2: Classification accuracy (%) of land use classes in various decomposition techniques

Decomp.→ Classes ↓	Freeman Durden	Moriy-ama	Eigen vector	H/A/ α
Urban	100	100	100	98.73
Crop	100	100	99.65	99.30
Scrub	96.86	97.42	96.18	80.47
Fallow land	98.16	98.51	99.50	92.32

Table 3: Overall classification accuracy and signature separability of various decomposition techniques for the selected land use classes

Decomp. Technique	Overall classification accuracy (%)	Overall signature separability
Freeman Durden	98.44	1390
Moriyama	98.74	1393
Eigen vector	99.11	1412
H/A/α	92.49	1345

Table 4: Ranking of different decomposition techniques for land use application

Rank No.	Overall classification accuracy	Overall separability
1	Eigen vector	Eigen vector
2	Moriyama	Moriyama
3	Freeman Durden	Freeman Durden
4	H/A/α parameter	H/A/α parameter

Figures 2, 3 and 4 show the FCC of decomposed images with red colour assigned to double bounce, green to volume scattering and blue to surface scattering. Figure 5 shows the H/A/α decomposed image of the study area. Classification accuracy of all land use classes were estimated for these decomposition techniques. Table-2 shows the results of classification accuracy of various land use classes.

On the basis of the overall classification accuracy, it was observed that urban and crop were classified better, as compared to scrub and fallow land, in all decomposition algorithms, due to more homogenous pixels as compared to the later two. Classification accuracy of urban class was 100% in case of Freeman, Moriyama and eigen vector, while in case of H/A/α it was 98.73%. Crops were best classified in case of Freeman Durden and Moriyama, followed by eigen vector and H/A/α decomposition. Scrub, as compared to other features was poorly classified, while the fallow land showed a similar trend of classification by various decomposition techniques as that of crops, except for the case of H/A/α decomposition.

Based on the results of the error matrix and class separability using Jeffries-Matusita distance, the polarimetric decomposition techniques were ranked for the land use class identification. Eigen vector based decomposition technique was found to be the best among four decomposition techniques under study. Freeman Durden and Moriyama decompositions performed nearly equal, being slightly lower than eigen vector decomposition. H/A/α decomposition performance was found to be comparatively poor. It showed good separability for urban and crop classes while poor in classifying Fallow and Scrub areas. Table 3 shows the overall classification accuracy and class separability for the various decomposition techniques and table 4 shows the ranking of these decomposition techniques based on results in table 3.

5. Conclusion

The present study was aimed for assessing the suitability of various decomposition techniques for land use classification. Among the various decompositions used in the study, best accuracy of classification and separability was observed for eigen vector based decomposition, followed by Moriyama decomposition, Freeman Durden decomposition and H/A/α decomposition. This study could further be extended in C-band and for other geographic areas to find out the suitable decomposition techniques for land use classification.

Acknowledgements

We express thanks to JAXA, Japan for providing us SAR data under Announcement of opportunity project.

References

Cloude, S.R. and E. Pottier (1996). A review of target decomposition theorems in radar polarimetry. IEEE Trans. GRS, vol. 34(2), pp. 498-518.

Das, A.K. (2011). SAR polarimetric analysis. RISAT-UP Training Programme on Radar Remote Sensing and Applications, 7th (14 – 25 February 2011), pp. 166-190.

Freeman, A. and S.L. Durden (1998). A three-component scattering model for polarimetric SAR data. IEEE Transactions on Geoscience and Remote Sensing, vol. 36,no. 3, pp. 963-973.

Lee, J.S., M.R. Grunes, E. Pottier and L. Ferro-Famil (2004). Unsupervised terrain classification preserving polarimetric scattering characteristics. IEEE Transactions onGeoscience and Remote Sensing, vol.42, no.4, pp. 722-731.

Moriyama, T. Y. Yamaguchi, M. Ishido, H. Yamada (2005). Four-component scattering model for polarimetric SAR image decomposition. IEEE Trans. Geoscience and Remote Sensing 43(8): 1699-1706.

Zhang, L., J. Zhang, B. Zou and Y. Zhang (2008). Comparison of methods for target detection and applications using polarimetric SAR image. PIERS Online, vol. 4, no.1, pp 140 - 145.